JCTC Journal of Chemical Theory and Computation

Article

pubs.acs.org/JCTC

Fe(III)−Heme Complexes with the Amyloid Beta Peptide of Alzheimer's Disease: QM/MM Investigations of Binding and Redox Properties of Heme Bound to the His Residues of Aβ(1−42)

Samira Azimi and Arvi Rauk*

Department of Chemistry, The University of Calgary, Calgary, Alberta, Canada T2N 1N4

Supporting Information

ABSTRACT: Pursuant to our previous paper [*J. Chem. Theory Comput.* **2012**, *8*, 5150−5158], the structures of complexes between Aβ(1−42) and ferriheme (Fe(III)−heme−H_2O) were determined by application of Amber and ONIOM-(B3LYP/6-31G(d):Amber) methodology. Attachment at each of the three His residues was investigated. As well as direct bonding of the iron to the His residue, bonding is augmented by formation of secondary salt bridges between the carboxylate groups of the heme and positively charged residues of Aβ (at His13, by Lys16 and the N-terminus; at His14, by Lys16; at His6, by Arg5). The results indicate a slight preference for His13 followed by His6 and His14, with the lowest 10 structures lying within 30 kJ mol^{-1} of each other. The absolute binding affinities are predicted to be approximately 30−40 kJ mol^{-1}. Standard reduction potentials (E°) are calculated for various Fe(III)/Fe(II) couples. Regardless of the point of attachment of the heme, E° values are approximately −0.6 V relative to the standard hydrogen electrode.

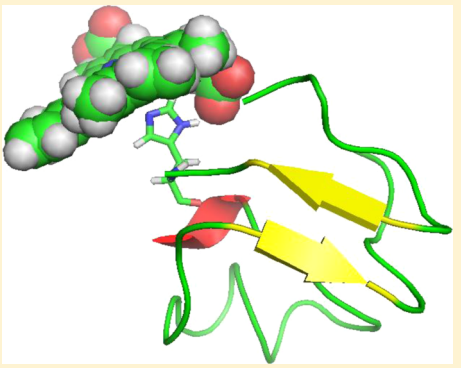

INTRODUCTION

Alzheimer's disease (AD) is characterized by the progressive and irreversible loss of neurons and synapses in the cerebral cortex resulting in long and short-term memory loss and disability in thinking and learning. The physiological markers are the appearance of intracellular tangles of an abnormal form of the tau protein, and extracellular plaques consisting primarily of the amyloid beta peptide (Aβ), and with elevated levels of copper, zinc, and iron. By current consensus, the neurotoxic agents are soluble oligomeric forms of Aβ, most likely associated with metal ions.

The sequence of Aβ(1−42), in single letter code, is

$$A\beta(1{-}42) = D_1AEFR_5\mathbf{H}DSGY_{10}EV\mathbf{H}$$
$$\mathbf{H}Q_{15}KLVFF_{20}AEDVG_{25}SNKGA_{30}IIGLM_{35}VGGVV_{40}IA$$

The mechanisms of neuronal toxicity of Aβ are complex and multifaceted, including interference with insulin and glutamate receptors at synapses, loss of calcium homeostasis, and inflammation and lipid peroxidation caused by various reactive oxygen (radicals) species (ROS). The association with metals accelerates oligomerization and, in the case of the redox active metals copper and iron, promotes ROS formation. It is this latter aspect, and iron specifically, that is the subject of the present study.

The predominant form of active iron is heme, the complex between Fe(III) or Fe(II) and protoporphyrin IX. Heme is a prosthetic group in numerous enzymes responsible for oxygen transport (hemoglobin) and redox activity (catalase, peroxidases, the cytochromes). Aβ has been shown to have two

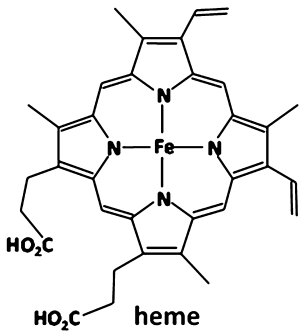

binding sites for heme,[1] in the hydrophilic domain, residues 1−16, and in the hydrophobic domain, residues 17−40/42. The binding to the hydrophobic domain has been questioned on the basis that interaction with Aβ(17−40) does not perturb the spectroscopic signature of heme.[2] This is not surprising, as there are no good ligands for the Fe of heme in this region, but does not obviate heme binding by another mechanism, such as salt bridging to Lys28 and/or π-stacking to the Phe residues. An investigation of heme binding to the lipophilic region of Aβ is beyond the scope of the present work. Atamna and co-workers have shown that Fe(III)−heme binds to Aβ with submicromolar affinity, implying that $\Delta G \approx -40$ kJ/mol.[4] This result was supported in a recent computational study of the binding of imidazole to Fe(III) porphine (a model for heme), $\Delta G = -44$ kJ/mol.[3] Electrostatic interactions between the negatively

Received: May 3, 2013

   dx.doi.org/10.1021/ct400364b | *J. Chem. Theory Comput.* XXXX, XXX, XXX−XXX

charged heme ($-1e$) and negatively charged Aβ ($-3e$) would act to weaken the interaction if it is not countered by attractive interactions between the two propylcarboxy groups and positively charged residues (N-terminus, Arg5, Lys16, or Lys28). Spectroscopic studies have partially resolved the nature of the binding of heme to Aβ.[2,4] Aβ has a Tyr residue so the binding *could* be of the catalase kind.[5] However, while inorganic Fe(III) binds to Tyr10,[6] Tyr10 has been shown not to be a ligand to the iron in heme.[2] Rather, His6, His13, and H14 have been confirmed as the principal binding sites for the heme, with a strong preference for His13. It was suggested that Arg5 plays an important role as a secondary binding component. The observed peroxidase-like activity also suggests that the heme should be attached to one of the three His residues.[7,8]

All of the His residues have been shown experimentally and theoretically to serve as binding sites for Cu^{2+}. However, spectroscopic evidence seems to suggest that ferriheme (Fe(III)−heme) and cupric ions (Cu^{2+}) bind to Aβ simultaneously and independently of each other.[9] These observations seem to contradict what is accepted about the nature of the coordination of copper to Aβ. Numerous experimental and theoretical studies[10−18] have shown that Cu^{2+} binds in the hydrophilic domain, principally at the His residues and the N-terminus, while cuprous ion (Cu^{+}) binds solely at His13 and His14. The complex pH-dependent nature of the Cu^{2+} binding has recently been clarified computationally on model systems.[19] The lower pH component (Component I) is associated with the N-terminus, His6, and one of His13 or His14. At higher more physiological pH, this component morphs into a second component (Component II) that is bound to all three His residues as well as an amide carbonyl oxygen atom of Ala2. The spectroscopic evidence of Pramanik, et al.,[2,9] that the presence or absence of heme make no difference to the binding of copper, and vice versa, has led the authors to conclude that the copper could not be bound to all three His residues. There is almost universal agreement that His6 is involved in Cu^{2+} binding in both Component I and Component II of Cu(II)/Aβ. At least, in the case of Component I, one of His13 or His14 could bind the heme and the other serve as a second ligand for the copper. However, it seems unlikely that the heme and Cu^{2+} could be bound independently to His13 and His14, since the two residues are in close proximity and some spectroscopic perturbation, including spin−spin coupling, should be evident. The alternative, that His13 and His14 are reserved for the copper and that His6 is the heme-binding site, would call into question the experimental data that suggest His6 to be involved in the Cu^{2+} binding in both Component I and Component II. However, this was the scenario we suggested for the fully *reduced* metal system on the basis of our previous investigation of Fe(II)−heme−Aβ,[19] and the fact that Cu^{+} binds to His13 and His14[20] with femtomolar affinity,[21] which is significantly higher than found for the binding of heme.[4] One objective of the present study is to assess computationally which of the His residues is the most likely site of attachment of Fe(III)−heme to Aβ.

Heme bound to the beta amyloid peptide has peroxidase activity.[1,9] The resting state of the heme in naturally occurring peroxidases is the Fe^{3+} form, which, in the accepted mechanism, itself acts as a *reducing* agent producing an Fe(IV) oxo species commonly referred as Compound I.[22,23] In the experiments of Atamna and Boyle[1] and of Xu, and co-workers,[24] which demonstrated peroxidase activity of the heme-Aβ complex, a strong reducing agent was not involved, and it is evident that the Fe^{3+} form can also act as a peroxidase, presumably following the accepted mechanism. The Cu^{2+}/Aβ complex also displays peroxidase activity: under reducing conditions in the presence of O_2, H_2O_2 is produced, and the H_2O_2 is further reduced to hydroxyl radicals. In the case of Cu^{2+}/Aβ, the redox chemistry proceeds through the *reduced* form of the metal, namely Cu^{+}/Aβ. In experiments to assess the peroxidase-like activity of heme−Aβ and heme−Aβ−Cu complexes, sodium dithionite (E° = −0.66 V vs SHE[25]) was used as a reducing agent to produce the ferro form.[9] A second objective of the present study is to assess whether the "peroxidase-like" activity of the heme−Aβ complex proceeds through the normal enzymatic mechanism and/or whether it follows the Cu^{+}/Aβ mechanism and proceeds through the Fe(II)−heme form.

In our previous study,[26] we found that the reduced Fe(II)−heme could bind to each of His6, His13, and His14, with a slight preference for the binding to His13 with binding affinity less than 70 kJ mol^{-1} ($\log_{10} K < 12$). The binding affinity of Cu^{+} to Aβ is substantially higher, $\log_{10} K = 14$,[27] and occurs at His13His14.[28] For this reason, we suggested that simultaneous binding of the *reduced* species, Cu^{+} and ferroheme, to Aβ is possible provided the heme is attached at His6. Since the binding affinity of Cu^{2+} to Aβ ($\log_{10} K \approx 9$)[29,30] is substantially less than that of Cu^{+}, it is possible that the binding patterns of the oxidized species may be different. A third objective of the present study is to examine the binding of the *oxidized* heme to Aβ to ascertain if there is a difference from that of the reduced species.

METHODS

Following procedures established previously,[26] all calculations were carried out with the Gaussian 09 (G09) suite of programs[31] on Fe(III)−heme−Aβ(1−42)−H_2O. The bulk of the initial calculations on the complete Aβ−heme system were carried out with the Amber force field.[32] As before, an "annealing" procedure was employed, in which the heme was attached to each of the His residues at fixed distances. The complex was optimized and the distance reduced in 1 Å steps from 6 Å to 2 Å, with Amber-optimization, after which it was reoptimized using the mixed quantum mechanical−molecular mechanical (QM/MM) methodology, ONIOM.[33,34] As before, validation of the Amber part of the study was performed by comparison with pure B3LYP/6-31G(d) calculations on the part of the system that would become the "QM" part, namely the 4-methylimidazole (MeIm) complex with Fe(III)−heme−H_2O. In a previous study of Fe(III)−porphine with a similar methodology, quartet ground electronic states were found for all systems with a mix of imidazole and water ligands.[3] Accordingly, the geometries of MeIm, Fe(III)−heme−H_2O in its quartet electronic state, and their adducts, also in the quartet state, were optimized at the B3LYP/6-31G(d) level of theory.[35] Since the hextet states of the systems lay only a few kJ mol^{-1} higher, the same systems were also reoptimized as hextets. Harmonic frequency analysis was conducted at the same level of theory in order to obtain zero-point vibrational energies, the entropy at 298 K, and thermal corrections to the enthalpy, also at 298 K. The zero point energy was scaled by 0.9806.[36] The entropy at 1 atm pressure was converted to 1 M standard state by the addition of $R \ln(1/24.465)$. The free energy of solvation, ΔG_{solv}, was obtained via the SCRF keyword with the default parameters for water as implemented in G09.[37] In addition, the missing dispersion energy in B3LYP was estimated by the DFT-

dx.doi.org/10.1021/ct400364b | J. Chem. Theory Comput. XXXX, XXX, XXX−XXX

Table 1. Calculated Data for Fe(III)−Heme−H_2O (Heme), 4-Methylimidazole (MeIm), and the Complex (Heme−MeIm, the QM Part), and Fe(III)−Heme−Aβ in Both Quartet and Hextet States

	energy[a] hartree	ZPVE hartree	$H_{298}°-H_0°$ kJ mol^{-1}	S_{298} J K^{-1} mol^{-1}	disp kJ mol^{-1}	ΔG_{solv} kJ mol^{-1}	ΔG_{aq} kJ mol^{-1}
MeIm	−265.53543	0.09923	16.7	281.7	−13.6	−27.3	
heme, quartet state	−3173.80007	0.59690	111.6	1011.1	−281.4	−266.1	0.0
heme, hextet state	−3173.80293	0.59573	112.7	1024.2	−278.6	−269.8	−14.1
heme−MeIm, quartet state	−3439.36741	0.69768	129.2	1129.8	−365.4	−245.6	0.0
heme−MeIm, hextet state	−3439.36289	0.69529	129.5	1132.1	−367.0	−232.7	16.6
Fe(III)−heme−Aβ (H13)A, quartet	−3441.10161	5.82877	969.2	7009.3	−356.3	−1613.30.0	
Fe(III)−heme−Aβ (H13)A, hextet	−3441.07447	5.82618	971.5	7041.8	−342.6	−1630.6	53.4

[a]Gaseous phase.

Table 2. Reaction Energies (kJ mol^{-1})[a]

reaction	ΔE	ΔZPVE	ΔDisp	ΔH_0	ΔH_{298}	$-T\Delta S$	$\Delta G_{(gas)}$	$\Delta\Delta G_{solv}$	$\Delta G_{(aq)}$
heme−MeIm ⇒ heme + MeIm[b]	76.3	−7.0	73.3	142.5	142.7	−52.5	90.2	−51.4	38.8
−Aβ(H13)**A**⇒ eq 1	−154.2	−11.6	−61.3	−101.7	−101.5	−56.9	−158.5	194.6	36.1

[a]ΔE = Born−Oppenheimer; ΔDisp = dispersion correction; ΔH_0, ΔH_{298} = enthalpy at 0 and 298 K; ΔS = entropy; ΔG(gas), ΔG(aq) = Gibbs free energy in gaseous and aqueous phases; $\Delta\Delta G_{solv}$ = free energy of solvation. [b]Heme−MeIm, Fe(III)−heme−Aβ(H13)**A**, and Fe(III)−heme (heme) are in their lowest electronic states, quartet, quartet, and hextet, respectively.

D3 procedure of Grimme and co-workers.[38] Details of the QM calculations are reported in Table 1. For Fe(III)−heme−H_2O, the hextet state is more stable than the quartet state by 14 kJ mol^{-1}. The reverse is true for Fe(III)−heme−MeIm−H_2O, the quartet state is more stable than the hextet state by 17 kJ mol^{-1}.

The Amber charges for the atoms in Fe(III)−heme−H_2O were taken as the CHELPG charges obtained from the B3LYP/6-31+G(d) wave function of the B3LYP/6-31G(d)-optimized geometry of the complex in its quartet state. A sample input file containing all of the parameters is included in Supporting Information. The initial structure of Aβ was taken from the molecular dynamics study of Raffa and Rauk.[39] In addition to the "annealing" process described for the Fe(II)−heme−Aβ study,[26] all of the conformations of the previously found Fe(II)−heme−Aβ complexes were converted to Fe(III)−heme−Aβ−H_2O and reoptimized at the ONIOM level of theory. Both procedures yielded novel binding configurations, and in such cases, the optimized Fe(III)−heme−Aβ−H_2O structures were reoptimized as the reduced species after removing the H_2O, thus yielding a few conformations that were not previously found. Optimization of each structure was invoked with the command, "ONIOM(B3LYP/6-31G-(d):AMBER=hardfirst)=embedcharge" . The "QM" part of the system corresponds to Fe(III)−heme−H_2O and the side chain of each His residue, converted into MeIm by the addition of a hydrogen to the β-C and linked mechanically to the α-C. The "embedcharge" keyword denotes that the Amber charges are seen by the "QM" system. The effect of implicit solvation by water was included at the IEFPCM level, as described above.[34] The dispersion part of the total energy missing from the B3LYP treatment of the QM part was estimated by the DFT-D3 procedure[38] and added to the total energy.

The lowest energy His13-bound structure of the Fe(III)−heme−Aβ−H_2O system was reoptimized in its hextet state and found to lie 53 kJ mol^{-1} higher in energy than the quartet state.

RESULTS

Structure of Aβ(1−42). The structure of Aβ(1−42) in water is not known from experiment, since it is fluxional on the time scale of NMR experiments. The structure for heme-free Aβ(1−42) was taken from our study of the reduced systems[26] and is based on a Gromacs MD simulation in water.[39] Docking of either the Fe(II)−heme[26] and Fe(III)−heme−H_2O in various orientations to His6, His13, and His14 did not induce a major conformational change in the Aβ skeleton.

Structure and Energetics of Fe(III)−Heme-4-Methylimidazole−H_2O (the "QM" Part). 4-Methylimidazole (MeIm) is a model for the side chain of the His residues. Experimentally, coordination of imidazole to Fe(III)−heme in water is very weak, $\Delta G \approx -20$ kJ mol^{-1}.[3,40,41] The Fe(III)−heme−MeIm−H_2O system is small enough so that all of the steps required to calculate the free energy of dissociation in water at 298 K for both the quartet and hextet states can be carried out at a reasonable level of theory. These include B3LYP/6-31G(d) optimization, harmonic frequency analysis, solvation correction by IEFPCM, and dispersion correction by DFT-D3. The primary data are given in Table 1. According to the calculations, the complete complex is in its quartet state but dissociates into MeIm and Fe(III)−heme−H_2O in a lower energy hextet state. We take this result at face value since the B3LYP functional has been shown to be generally reliable for the prediction of the ordering of the spin states of iron porphyrins.[42] The data for the reaction between the heme and MeIm are listed in Table 2. The free energy of binding of MeIm to Fe(III)−heme at 298 K in water is calculated to be ΔG = −39 kJ mol^{-1}, in reasonable agreement with experiment and previous ab initio calculations on model systems.[3] We conclude from these results that the approximate methodology that must be applied, namely QM/MM (B3LYP/6-31G(d) /Amber), with solvation, thermal, and dispersion corrections, is adequate to describe the Fe(III)−heme−Aβ−H_2O system.

New Structures of Fe(II)−Heme Bound to Aβ at His6, His13, and His14. In the naming system used below and in the rest of the paper, the presence of H_2O is understood for the Fe(III) species, and we assign bold lower- and upper-case letters to distinguish between Fe(II) and Fe(III) species, respectively. As well as the Fe(III)−heme−Aβ−H_2O structures, Table S1 of Supporting Information lists all of the primary computed energy data as well as key structural information for 10 isomers of the Fe(II)−heme−Aβ system, which had not been found in the earlier study but lie in a similar energy range.

dx.doi.org/10.1021/ct400364b | J. Chem. Theory Comput. XXXX, XXX, XXX−XXX

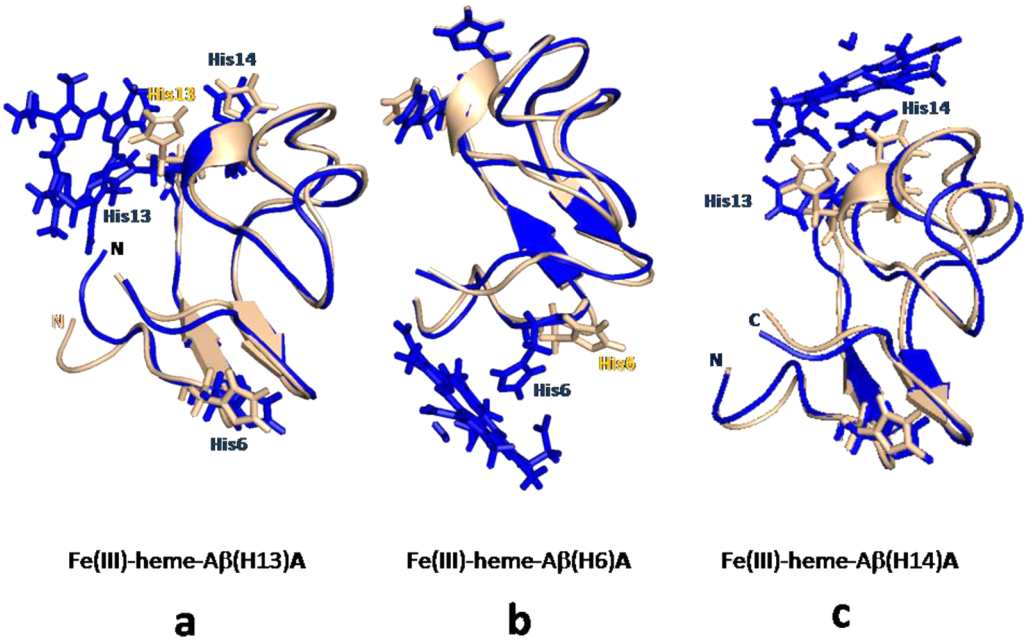

Figure 1. Cartoon representations of the Amber-optimized Aβ(1−42) (creamy white) superimposed on the three most stable ONIOM-optimized structures of complexes (blue): (a) Fe(III)−heme−Aβ (H13)**A**; (b) Fe(III)−heme−Aβ (H6)**A**; (c) Fe(III)−heme−Aβ (H14)**A**.

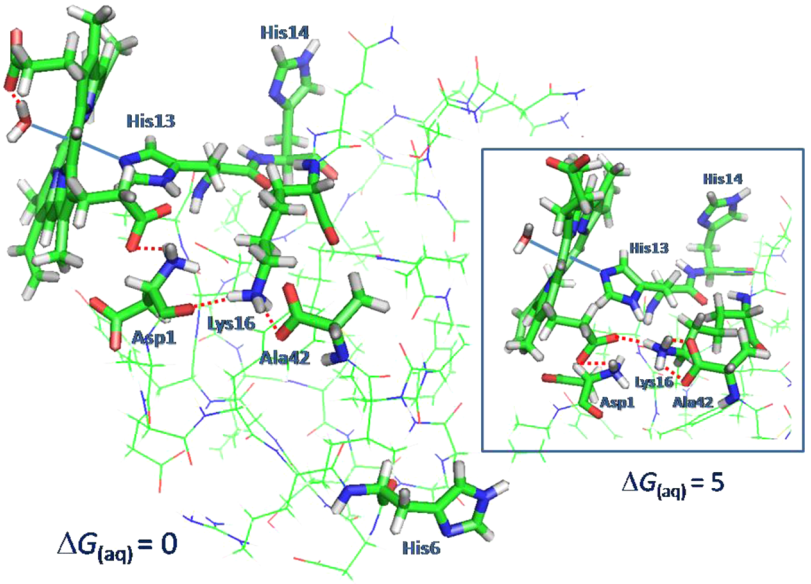

Figure 2. ONIOM-optimized structures of Fe(III)−heme−Aβ (H13)**A** and Fe(III)−heme−Aβ (H13)**B** (inset) showing details of the bonding environment of the heme. The heme group and the side chain of His13 constitute the QM part. ΔG(aq) values are relative to Fe(III)−heme−Aβ(H13)**A**.

All of the structures are higher in energy that the most stable structure, Fe(II)−heme−Aβ(H13)**a**. However, lower energy structures, denoted by primes (′) were found for both the His14-bound heme and the His6-bound heme. The lowest His14-bound structure, Fe(II)−heme−Aβ(H14)**a**′ is 17 kJ mol^{-1} above Fe(II)−heme−Aβ(H13)**a** rather than 31 kJ mol^{-1} (Fe(II)−heme−Aβ(H14)**a**). The lowest His6-bound structure, Fe(II)−heme−Aβ(H6)**a**′ is 22 kJ mol^{-1} above Fe(II)−heme−Aβ(H13)**a** rather than 28 kJ mol^{-1} (Fe(II)−heme−Aβ(H6)**a**). Some of these structures are important in the redox chemistry of the heme−Aβ system and are discussed further in the following text.

Structures of Fe(III)−Heme−H_2O Bound to Aβ at His6, His13, and His14. Table S2 of Supporting Information lists all of the primary computed energy data as well as key structural information for the 18 isomers of the Fe(III)−Heme−Aβ−H_2O system that had relative aqueous free energy under 70 kJ mol^{-1}, in decreasing order of stability. The last column indicates the root-mean-square deviation (rmsd) of all of the atoms of the Aβ backbone of the Amber-optimized structure, and the ONIOM-optimized structure. All of the rmsd values are within 2 Å, indicating that there is no major change in the Aβ conformation upon attachment of the heme, regardless of where the heme is attached. This is illustrated graphically in Figure 1 where the Amber-optimized Aβ structure (pale cream)

dx.doi.org/10.1021/ct400364b | J. Chem. Theory Comput. XXXX, XXX, XXX−XXX

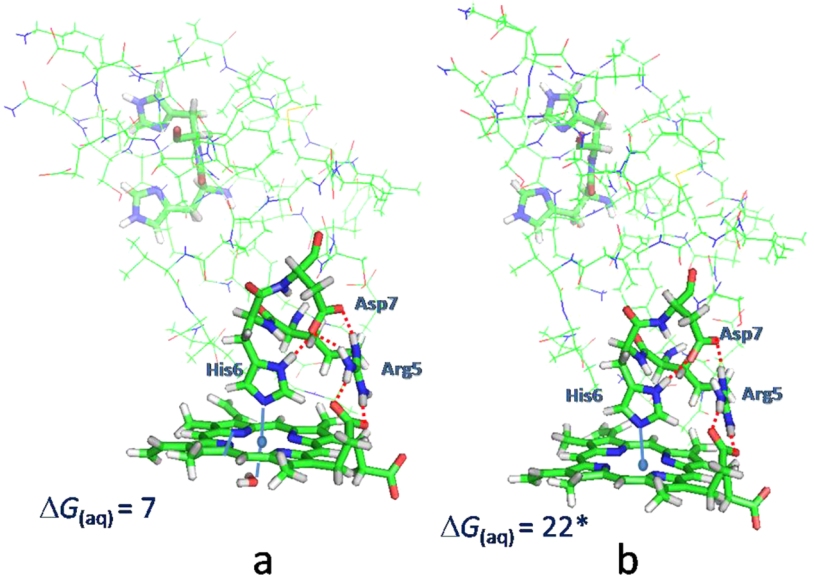

Figure 3. (a) ONIOM-optimized structure of Fe(III)−heme−Aβ (H6)**A** showing details of the bonding environment of the heme. Arg5 forms a salt bridge to one of the heme carboxylate groups. The ΔG(aq) value is relative to Fe(III)−heme−Aβ (H13)**A**. The heme group and the side chain of His6 constitute the QM part. (b) ONIOM-optimized structure of Fe(II)−heme−Aβ (H6)**a′** showing the similarity of the bonding to Fe(III)−heme−Aβ(H6)A.

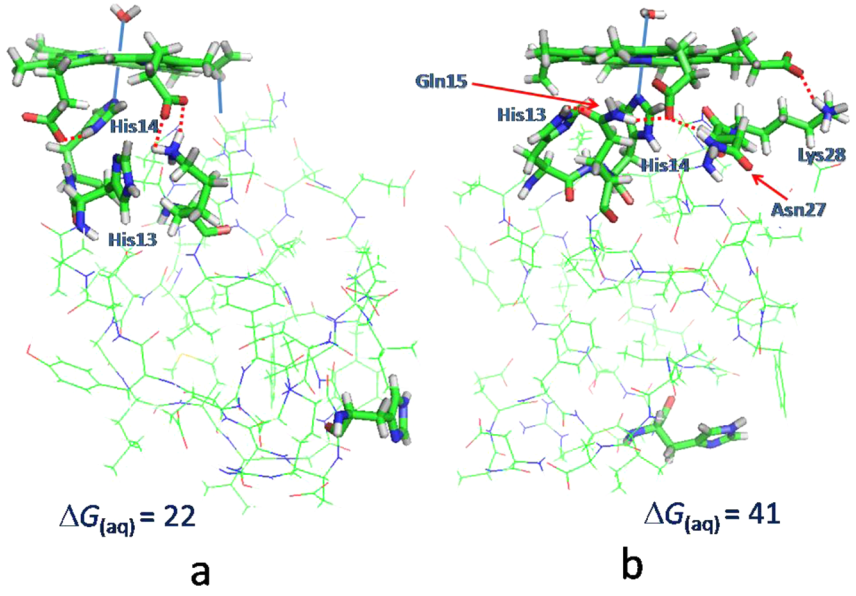

Figure 4. ONIOM-optimized structures of (a) Fe(III)−heme−Aβ (H14)**A**; and (b) Fe(III)−heme−Aβ(H14)**B** showing details of the bonding environment of the heme. The heme group and the side chain of His14 constitute the QM part. ΔG(aq) values are relative to Fe(III)−heme−Aβ(H13)**A**.

is compared to the ONIOM-optimized structure (blue) in cartoon representation. The lowest energy complex of each type is shown. The most stable structure, Fe(III)−heme−Aβ(H13)**A** (Figure 2), is one in which the heme is attached to His13. It is approximately 5 kJ mol^{-1} more stable than the next lowest His13-bound system, Fe(III)−Heme−Aβ(H13)**B** (Figure 2 inset), 7 kJ mol^{-1} more stable than the lowest His6-bound system, Fe(III)−heme−Aβ(H6)**A** (Figure 3a), and 22 kJ mol^{-1} lower than the lowest His14-bound complex, Fe(III)−heme−Aβ(H14)**A** (Figure 4). Two more His13-bound structures, Fe(III)−heme−Aβ(H13)**C**, Fe(III)−heme−Aβ-(His13)**D**, and a His6-bound Fe(III)−heme−Aβ(H6)**B**, are below the lowest His14-bound species. In all, six structures lie in the range 0−20 kJ mol^{-1}. In view of the approximations in the methodology, it is not possible to assign with confidence relative energies of structures that lie in such close proximity of each other.

The explicit heme bonding details of the eight lowest energy structures are shown in Figures 2−4. In the most stable structure, Fe(III)−heme−Aβ(H13)**A** (Figure 2), one of the propylcarboxylate groups of the heme is involved in a salt bridge with the N-terminal Asp1. The side chain of Lys16 has extended to reach the carboxylate group of Asp1, and also to the C-terminus. Significant displacements of the N-terminus and the side chain of His13 with its pendant heme has brought the two moieties close enough to allow the N-terminal Asp1 to

dx.doi.org/10.1021/ct400364b | J. Chem. Theory Comput. XXXX, XXX, XXX−XXX

Table 3. Reduction Potentials for Various "Fe(III)"/"Fe(II)" Couples[a]

"Fe(III)" + e ⇒ "Fe(II)"	ΔH_0	$_{\Delta}H_{298}$	$-T\Delta S$	$\Delta G_{(gas)}$	$_{\Delta\Delta}G_{solv}$	$_{\Delta}G_{(aq)}$	E°	rmsd	ΔG^{FeIII}	$^{\Delta}G^{FeII}$
(H6)**A** ⇒ (H6)**a**′	220.6	220.8	−34.3	186.5	−525.4	−338.9	**−0.82**	0.98	0.0	0.0
(H6)**D** ⇒ (H6)**a**	229.6	233.0	−44.2	188.7	−542.3	−353.6	**−0.67**	0.09	21.3	6.6
(H6)**C** ⇒ (H6)**c**″	288.5	290.6	−37.6	253.0	−594.4	−341.3	**−0.79**	0.11	21.2	18.7
(H13)**A** ⇒ (H13)**a**	168.5	171.5	−30.1	141.5	−494.6	−353.2	**-0.67**	1.74	0.0	0.0
(H13)**A** ⇒ (H13)**b**	217.2	217.5	−25.7	191.8	−521.5	−329.7	**−0.92**	0.50	0.0	23.5
(H13)**B** ⇒ (H13)**a**	224.5	228.7	−43.8	184.9	−542.9	−358.0	**−0.62**	0.40	4.8	0.0
(H13)**C** ⇒ (H13)**b**	229.8	232.7	−35.2	197.6	−539.6	−342.0	**-0.79**	0.35	12.4	23.5
(H14)**A** ⇒ (H14)**a**′	112.4	112.8	−1.8	111.1	−469.4	−358.4	**−0.62**	2.40	0.0	0.0
(H14)**B** ⇒ (H14)**a**′	166.8	169.3	−35.6	133.7	−511.0	−377.3	**−0.42**	0.19	18.9	0.0
(H14)**D** ⇒ (H14)**a**″	167.8	176.0	−57.3	118.7	−513.8	−395.2	**−0.24**	0.46	44.5	7.8
(H14)**D** ⇒ (H14)**a**	174.4	182.6	−57.9	124.7	−513.6	−388.9	**−0.30**	0.45	44.5	14.0

[a]Reaction energies (kJ mol^{-1}): ΔH_0, ΔH_{298} = enthalpy at 0 and 298 K; ΔS = entropy; ΔG(gas), ΔG(aq) = Gibbs free energy in gaseous and aqueous phases; $\Delta\Delta G_{solv}$ = free energy of solvation; E° = reduction potential in Volts relative to SHE; rmsd Å between "Fe(III)" and "Fe(II)"; ΔG_{FeIII}, ΔG_{FeII} = free energies relative to the most stable oxidized and reduced species, respectively.

make the two salt bridges. The displacement of the N-terminus is evident in the cartoon representations in Figure 1a. A similar bonding and salt bridge configuration as Fe(III)−heme−Aβ(H13)**A** is present in the second structure, Fe(III)−heme−Aβ(H13)**B** (Figure 2 inset), 5 kJ mol^{-1} higher than the first. Fe(III)−heme−Aβ(H13)**B** differs mainly in a different orientation of the Asp1 side chain such that the heme carboxylate group forms salt bridges simultaneously to the N-terminus and to Lys16. In the next structure, Fe(III)−heme−Aβ(His13)**C** (not shown), which is 12 kJ mol^{-1} higher, the carboxylate of Glu11 makes a competing salt bridge to Lys16 and also to the N-terminus. In addition, the second heme carboxylate has turned to make a H-bond to the bound water of the heme. The next His13-bound structure, Fe(III)−heme−Aβ(His13)**D** (not shown), at 18 kJ mol^{-1}, has a different bonding arrangement. The C-terminus bridges both the N-terminus and Lys16, but the heme propylcarboxylate is not involved. Instead, the second heme propylcarboxylate group makes a H bond to the N_{δ}−H of His13.

The two lowest energy structures in which the heme is attached to His6, Fe(III)−heme−Aβ(H6)**A** and Fe(III)−heme−Aβ(H6)**B**, lie 7 and 11 kJ mol^{-1}, respectively, above Fe(III)−heme−Aβ(H13)**A**. The former is shown in Figure 3a. They have the same bonding configuration of the His6 side of the heme. Arg5 simultaneously hydrogen bonds to Asp7 and one of the heme carboxylate groups. Asp7 also H-bonds to N_{δ}−H of His6. The two differ in that the second heme carboxlate group is out in solution in the case of Fe(III)−heme−Aβ(His6)**A** (Figure 3a) and has turned to H-bond to the distal bound water in the case of Fe(III)−heme−Aβ(His6)**B** (not shown). In our previous study, we did not find direct involvement of Arg5 in coordinating the Fe(II)−heme at His6 in any of the lower-lying structures.[26] However, reoptimization from Fe(III)−heme−Aβ(H6)**A** yielded Fe(II)−heme−Aβ(H6)**a**′ (Figure 3b) with almost identical bonding configuration. One notes that Arg salt bridging to heme is a common theme in heme proteins.[43]

The lowest energy His14-bound structure, Fe(III)−heme−Aβ(H14)**A** (Figure 4a), is 22 kJ mol^{-1} higher in energy than Fe(III)−heme−Aβ(H13)**A**. Both propylcarboxylate groups of the heme are involved in bonding. The side chain of Lys16 makes a salt bridge with one of the carboxylate groups. The second carboxylate group makes a H-bond with the N_{δ}−H of His14, causing the imidazole moiety to tilt away from being perpendicular to the heme plane. In the second lowest His14-bound structure (Figure 4b), again, both carboxylate groups are involved, one making a salt bridge with Lys28 and the other H-bonded to the side chains of both Gln15 and Asn27. His13 also H-bonds to Gln15 but is not directly interacting with the heme group.

Binding Affinity of Fe(III)−Heme Bound to Aβ at His13. The binding affinity of ferriheme to Aβ was assessed by calculating the free energy change in water for reaction 1:

$$\text{Fe(III)−heme−A}\beta\text{(H13)}\mathbf{A}\text{−}H_2O \Rightarrow \text{Fe(III)−heme−}H_2O + A\beta_{(H6)} \quad (1)$$

Both quartet and hextet states were considered. The data for the heme−Aβ complex and for Fe(III)−heme (heme) are listed in Table 1. One notes that the hextet state is the ground state of Fe(III)−heme−H_2O while for Fe(III)−heme−Aβ(H13)**A**−H_2O it is the quartet state. In the *reaction*, the QM part is separated, requiring an ONIOM calculation on Aβ with only the His side chain defined as the QM part. In our previous study, several ONIOM optimizations were carried out with the QM part defined as each of the His side chains, yielding A$\beta_{(H6)}$, A$\beta_{(H13)}$, and A$\beta_{(H14)}$.[26] The lowest free energy in solution was found for A$\beta_{(H6)}$, the structure with His6 as the QM part. Accordingly, A$\beta_{(H6)}$ is used as the heme-separated product in reaction 1.

The raw data for the calculation of the binding affinity according to eq 1 are given in Table 1. Table 2 provides the computed details for the reaction. One can see from the column ΔH_0 or $\Delta G_{(gas)}$ of the second row of Table 2 that Fe(III)−heme−Aβ(H13)**A**−H_2O is not predicted to be stable in the gaseous phase. This is not surprising, since the high charge of the system, $-4e$, is assembled from Aβ with charge of $-3e$ and Fe(III)−heme−H_2O with charge of $-1e$. The change in free energy of solvation, $\Delta\Delta G_{solv}$ = 195 kJ mol^{-1}, is large and positive and more than compensates for the gaseous phase repulsion. The predicted binding energy, $\Delta G_{(aq)}$, of the most stable structure, Fe(III)−heme−Aβ(H13)**A**−H_2O, is 36 kJ mol^{-1}. This value is lower than previously found for Fe(II)−heme−Aβ(H13)**a**, 69 kJ mol^{-1} by the same procedure, and is in good agreement with the value of Atamna et al. for the binding of Fe(III)−heme to Aβ, 40 kJ/mol.[4] From the relative energies listed in Supporting Information Table S1 and in Figures 3 and 4, one can deduce that the binding affinities of Fe(III)−heme bound to His6 and His13 are 29 kJ mol^{-1} and 14 kJ mol^{-1},

dx.doi.org/10.1021/ct400364b | J. Chem. Theory Comput. XXXX, XXX, XXX−XXX

respectively. These are significantly lower than for Fe(II)−heme, 41 kJ mol^{-1} and 38 kJ mol^{-1}, respectively.[26]

Reduction Potentials of Fe(III)−Heme Bound to Aβ at His13, His6, and His14. Standard reduction potentials, $E°$, relative to SHE are calculated from the aqueous free energy changes for reaction 2:

$$\text{“Fe(III)”} + \frac{1}{2}\text{H}_2 \Rightarrow \text{“Fe(II)”} + \text{H}^+ \qquad \Delta G \tag{2}$$

where “Fe(III)” and “Fe(II)” represent the oxidized and reduced heme−Aβ species, respectively. The free energy change is assembled from the free energy changes for the half reactions 3 and 4, ignoring the electron:

$$\text{“Fe(III)”} + e \Rightarrow \text{“Fe(II)”} \qquad \Delta G^{\text{Fe}} \tag{3}$$

$$\frac{1}{2}\text{H}_2 \Rightarrow \text{H}^+ + e \qquad \Delta G^{\text{SHE}} \tag{4}$$

Thus, $\Delta G = \Delta G^{\text{Fe}} + \Delta G^{\text{SHE}}$, where ΔG^{SHE} = 418 kJ mol^{-1},[44] and $E° = -\Delta G/F$, where F is the Faraday constant, 96.485 kJ mol^{-1} V^{-1}. Table 3 lists calculated $E°$ values for a variety of “Fe(III)”/“Fe(II)” couples, together with rmsd values between the oxidized and reduced species (excluding the H_2O). Electron transfer between “Fe(II)” and “Fe(III)” will be fastest if the conformations of the two species are most similar (lowest rmsd values). Thus, the reduction potential is determined from thermodynamic considerations only if the oxidized and reduced species are in their most stable conformations when the electron is attached. Otherwise, the measured value and the rate of electron transfer will depend on pre- and/or postequilibria as in the case of Cu/Aβ(1−16).[19,45] All of the calculated $E°$ values in Table 3 are negative, for the most part, −0.6 V or lower. Cyclic voltametric (CV) measurements on heme−Aβ complexes have peak current values on the vicinity of −0.2 V[24] so the much lower values obtained are probably due to systematic errors in the theoretical treatment. This observation is considered in the Discussion.

DISCUSSION

In this follow-up investigation of the interactions of heme with Aβ, we have studied the oxidized ferriheme (Fe(III)−heme) and discuss its redox chemistry. As in the previous study,[26] the His residues not involved in the binding of heme were kept in the neutral state. This is the major component at physiological pH = 7.4, since the pK_a of histidine is 6.2 and the pK_a values of the His residues of Aβ(1−28) are close to 6.5 (by NMR in D_2O).[46] Also, as previously explained, the large size of the system required that QM/MM geometry optimization be carried out in the gaseous phase despite the high charge (−4e). All of the Fe(II)−heme−Aβ structures found earlier were converted to Fe(III)−heme−Aβ-H_2O and reoptimized. In some cases, new bonding motifs arose and these “Fe(III)” structures were cycled back to “Fe(II)” structures by addition of an electron and removal of the bound water (which does not remain coordinated to reduced iron). The large QM region (85 atoms) required a fairly modest ab initio approach, B3LYP/6-31G(d), in the QM/MM calculations. Because the ONIOM methodology cancels out the MM energy component of the QM part, the dispersion contribution to the energy that is integral to the MM (Amber) force field but lacking in B3LYP was also subtracted out and needed to be replaced by the empirical DFT-D3 procedure of Grimme.[38] Single point harmonic frequency analysis, and the implicit solvation by the IEFPCM procedure, afforded the determination of aqueous free energies at 298 K, from which binding affinities and standard reduction potentials were derived.

All calculations were performed on the quartet states of the Fe(III)−heme−Aβ system on the basis that the quartet state was the ground state for Fe(III)−porphine with water or imidazole substituents.[3] Additionally, calculations on the lowest hextet state of Fe(III)−heme−MeIm−H_2O and Fe(III)−heme−Aβ(H13)−H_2O (Table 1) confirmed that the quartet state was lower by 17 and 53 kJ mol^{-1}, respectively. On the other hand, the hextet state of Fe(III)−heme−H_2O was lower than the quartet state by 14 kJ mol^{-1}. The results obtained at the present theoretical level differ from EPR experiments at 77 K on Fe(III)−heme−Aβ(1−16) and Fe(III)−heme−Aβ(1−40), which clearly show a high-spin signal.[9] We cannot prove or disprove the fact that the difference is due to the solution state, solid vs liquid, or temperature 77 K vs 298 K.

In the end, 18 Fe(III)−heme−Aβ−H_2O structures, and nine additional Fe(II)−heme−Aβ structures with relative aqueous free energies below 70 kJ mol^{-1} were found. The computed data for these are listed in Table S2 of Supporting Information. As in the case of the Fe(II)−heme system, the most stable structure in aqueous solution is one in which the heme moiety is attached to His13 of Aβ(1−42) (labeled Fe(III)−heme−Aβ(H13)**A** in Figures 1 and 2a). Fe(III)−heme−Aβ(H6)**A** and Fe(III)−heme−Aβ(H14)**A** are only 7 and 22 kJ mol^{-1} higher, respectively.

Some bonding motifs in the oxidized systems were similar to those found earlier for the reduced system. At His13, the attachment of the iron atom to the imidazole was augmented by formation of salt bridges between one of the heme carboxylate groups and both the N- and C-termini, and Lys16 (Figure 2). A new pattern not previously found for the reduced system emerged when the oxidized heme approached His6. Arg5 formed salt bridges to both Asp7 and one of the heme carboxylates (Fe(III)−heme−Aβ(H6)**A**, Figure 3a). Reoptimization of this structure in reduced form yielded a lower energy structure with similar bonding (Fe(II)−heme-Aβ(H6)**a′**, Figure 3b) that is 6 kJ mol^{-1} more stable than that previously found. There has been some controversy about the importance of Arg5 to the bonding of heme to Aβ. Atamna et al. subjected Fe(III)−heme to varying amounts of human Aβ (huAβ) and rodent Aβ (roAβ) and determined the binding constants from the observed spectral changes.[4] Rodent Aβ differs from human Aβ in three genetic mutations, Arg5Gly, Tyr10Phe, and His13Arg. Their conclusions regarding the importance of Arg5 and His13, and the nonimportance of His6 and His14, in the binding were inferred from the observation that roAβ binds heme much less strongly than huAβ, since the former lacks Arg5 and His13 but contains His6 and His14. Our findings are not inconsistent with these observations. We find a small preference for His13 over His6 for binding of Fe(III)−heme. Arg5 plays a role in the binding of heme to His6 (see Figure 3), which may explain why roAβ binds heme much less strongly—it has His6 but not Arg5. Subsequently, Pramanik and Dey[2] proposed an alternative role for Arg5 in the binding of heme to His13 through hydrogen bonding to the coordinated distal water molecule, which is also important for its peroxidase activity.

Coordination of Fe(III)−heme−H_2O at His14 emerges as the least favorable. The lowest energy isomer, Fe(III)−heme−Aβ(H14)**A** (Figure 4a) is 22 kJ mol^{-1} less stable than the His13-bound isomer. Both heme carboxylates are involved in

dx.doi.org/10.1021/ct400364b | J. Chem. Theory Comput. XXXX, XXX, XXX−XXX

interactions with Aβ. One makes a H-bond to the N^{δ}−H of His14, tilting it substantially away from the perpendicular arrangement. The other makes a salt bridge to Lys16.

Five structures, Fe(III)−heme−Aβ(His13)**A**,**B**,**C**, and Fe(III)−heme−Aβ(His6)**A**,**B** lie within 12 kJ mol^{-1} of each other. Because of the nature of the approximations in the model chemistry, it is not possible to say with certainty which of His6 or His13 preferentially binds the heme, but His14 seems not to be a candidate. The same uncertainty pertains to the calculated binding energy. The most stable structure, Fe(III)−heme−Aβ(His13)**A** is predicted to be bound by 36 kJ mol^{-1} (Table 2), a value in good agreement with the experimental value for Fe(III)−heme−Aβ(1−42), 40 kJ mol^{-1}. The lowest His6-bound structure is only 7 kJ mol^{-1} less stable, 29 kJ mol^{-1}. Given the relatively low and similar binding affinities of the His13- and His6-bound species, it is likely that Fe(III)−heme−Aβ exists as a mixture of the two species. If Cu^{2+} is introduced to the Fe(III)−heme−Aβ system, the copper would shift the equilibrium to the His6-bound heme and attach to His13His14. If Cu^{2+} is already present and bound to all three His residues as in Component II, the heme would have to competitively remove one of the His residues, say His6, from the Cu^{2+} coordination sphere. In the recent theoretical study of Cu^{2+} binding to *models* of Aβ,[19] we found that loss of an imidazole (representing His6) leaving the copper attached to His13His14 required only 12.5 kJ mol^{-1}. Since the binding of Fe(III)−heme to His6 is predicted to be about 29 kJ mol^{-1}, it is plausible that a complex of Aβ with both heme and copper could exist as suggested by Pramanik, et al.[2,9] Attachment of Cu^{2+} to His13−His14 is compatible with the attachment of the heme at His6. However, it is difficult to see why the presence of one would not show up as a spectroscopic perturbation of the other.

We also concluded in our previous study of Fe(II)−heme−Aβ that the *reduced* heme should be attached to His6 in the presence of Cu^{+} on the basis that Cu^{+} has a much higher affinity for Aβ when coordinated to His13−His14 in a linear fashion. Thus, the redox chemistry of the heme−Aβ−Cu system should be efficient and reversible since the complex does not have to undergo a major conformational change upon reduction or oxidation.

Standard Reduction Potentials, *E*°, of Heme−Aβ Complexes. The calculation of reduction potentials by eqs 2 and 3 is especially challenging because the free energies of open shell species of different charges in aqueous solution must be determined to an accuracy of a few kJ mol^{-1}. Realistically, our procedures entail an uncertainty in $\Delta G_{(aq)}$ of about 20 kJ mol^{-1} for species within the same oxidation state. For processes in which the oxidation state changes, the uncertainty rises to 40 kJ mol^{-1}, which corresponds to an uncertainty of 0.4 V in *E*°, In addition, there is a bias toward more negative values as compared to experimental CV traces on various heme−Aβ complexes.[24] Table 3 lists *E*° values for several redox couples for each of His6-, His13-, and His14-bound complexes. The first row in each group corresponds to redox cycling between the most stable Fe(III) and Fe(II) species. The others correspond to redox reactions between higher energy species that are closest to each other in structure based on rmsd comparison of their coordinates. Pairs connected by the smallest rmsd values will add or lose electrons most efficiently and the observed *E* value will be weighted toward their *E*° values. All of the *E*° values listed in Table 3 are negative and most fall in at values −0.6 V or lower. Even if these values are too negative by as much as 0.4 V, it is clear that the Fe(III)−heme−Aβ complexes are difficult to reduce and the resting state will be the Fe(III)−heme−Aβ form. In the context of the in vitro experiments, peroxidase activity depends on the ability to reduce oxygen to superoxide ($O_2 + e^- \rightarrow O_2^{\bullet -}$, $E^\circ = -0.33$ V)[47] and hydrogen peroxide to hydroxyl radical ($H_2O_2 + e^- + H^+ \rightarrow H_2O + OH^{\bullet}$, $E^\circ = +0.38$ V at pH 7).[47] The calculated and measured reduction potential of Fe(III)−heme−Aβ is negative and close to naturally occurring peroxidases, $E^\circ \approx -0.3$ V (horse radish peroxidase (HRP)).[22,23] Thus, the reduced form, Fe(II)−heme−Aβ, is able to reduce both H_2O_2 and O_2. By analogy with HRP, it is reasonable that Fe(III)−heme−Aβ can also reduce both oxygen species, that is, to exhibit peroxidase activity by the normal enzymatic mechanism as described in the Introduction. We have not investigated the further oxidation pathways of Fe(III)−heme−Aβ.

Reduction of Fe(III)−heme−Aβ to the Fe(II)−heme−Aβ species requires the action of a reducing agent with a reduction potential of at least −0.6 V. Pramanik et al. used sodium dithionite ($E^\circ = -0.66$ V vs SHE[48]) as the reducing agent to produce the ferro form in their experiments to assess the peroxidase-like activity of heme−Aβ complexes.[9] The Aβ−Cu^{2+} complex can also function as a peroxidase after reduction.[9] When separate equivalent amounts of Aβ(1−16)/Fe(III)−heme and Aβ(1−16)/Cu^{2+} were reduced and exposed to air, equivalent stoichiometric amounts (≈ 90%) of H_2O_2 were produced. The source of the second electron necessary for the reduction of O_2 to H_2O_2 was probably Tyr10. When the putative Aβ(1−16)/Fe(III)−heme/Cu^{2+} complex was treated in the same way, more than stoichiometric (≈ 130%) amounts of H_2O_2 were produced.[9] This result is evidence that a 1:1:1 complex of the *reduced* metal species is formed. At least computationally, the only reasonable candidate structure is one in which the Cu^{+} is bound to His13 and His14 while the Fe(II)−heme is bound at His6. In the absence of Cu^{+}, the most likely binding site for Fe(II)−heme is not His6 but rather His13. The present results on the *oxidized* system support a similar binding pattern for Fe(III)−heme if Cu^{2+} is present. However, in the absence of Cu^{2+}, the Fe(III)−heme can bind to His13 or His6 with equal probability within the expected uncertainly.

CONCLUSIONS

The structures of complexes between Aβ(1−42) and ferriheme (Fe(III)−heme) were determined by application of QM/MM theoretical methodology, specifically ONIOM(B3LYP/6-31G(d):Amber). Attachment at each of the three His residues was investigated. The results indicate an equivalent preference for His13 and His6. In all, six His13- or His6-bound structures lie in the range 0−20 kJ mol^{-1} below the lowest His14-bound structure at relative energy, 22 kJ mol^{-1}. The methodology is not precise enough to permit a definitive statement as to the relative stabilities nor to the absolute binding affinities. However, it is likely that the ferriheme would be distributed approximately equally among His13 and His6 in the absence of Cu^{2+}. In each case, direct bonding of the iron to the His residue is augmented by formation of secondary salt bridges between the carboxylate groups of the heme and positively charged residues of Aβ (at His13, by Lys16 and the N-terminus; at His6, by Arg5 and Asp7; at His14, by both Lys16 and Lys28), The multipoint attachment may reduce the formation of neurotoxic oligomers and fibrils by stabilizing a conformation that cannot oligomerize.

The present study cannot resolve the apparent contradictory assertions in the literature as to the nature of binding of ferriheme (Fe(III)−heme) to Aβ in the presence of Cu^{2+}. These assert on the one hand that ferriheme and Cu^{2+} can bind simultaneously and independently to Aβ, and on the other hand indicate that Cu^{2+} coordinates to at least two and probably all three His residues, leaving no room for the heme to attach in a fashion that would not perturb the Cu^{2+} coordination. The present results suggest that binding of the Fe(III)−heme is equally likely at His6 and His13 and less likely at His14. The most probable bonding configuration in the presence of Cu^{2+} is one in which Fe(III)−heme is attached to His6 while Cu^{2+} coordinates to His13 and His14. This configuration is equivalent to that proposed for Fe(II)−heme in the presence of Cu^{+} and permits the reduction of both metals without invoking a major rearrangement in geometry of the complex.

The calculated reduction potential, $E°$, is negative relative to SHE, possibly as low as −0.6 V. Thus, the heme-Aβ complex can act as a peroxidase in its Fe(III) form as well as its Fe(II) form, in agreement with experiments.

■ ASSOCIATED CONTENT

Ⓢ Supporting Information

Complete Gaussian 09 input file for ONIOM-optimization of Fe(III)−heme−Aβ(H13)**A** in Table S1. The coordinates are for the optimized structure. Table S2, calculated data for the lowest energy Fe(III)−heme−Aβ(1−42) structures and new Fe(II)-Aβ(1−42) structures. This information is available free of charge via the Internet at http://pubs.acs.org. Coordinates of the other structures are available from the authors by request.

■ AUTHOR INFORMATION

Corresponding Author

*E-mail: rauk@ucalgary.ca.

Notes

The authors declare no competing financial interest.

■ ACKNOWLEDGMENTS

We are grateful to the Natural Sciences and Engineering Research Council of Canada (NSERC) for financial support of this work and to Compute Canada and Westgrid for generous allocations of computational resources.

■ REFERENCES

(1) Atamna, H.; Boyle, K. *Proc. Natl. Acad. Sci. U.S.A.* **2006**, *103*, 3381−3386.
(2) Pramanik, D.; Dey, S. G. *J. Am. Chem. Soc.* **2011**, *133*, 81−87.
(3) Wondimagegn, T.; Rauk, A. *J. Phys. Chem. B* **2011**, *115*, 569−579.
(4) Atamna, H.; Frey, W. H., II; Ko, N. *Arch. Biochem. Biophys.* **2009**, *487*, 59−65.
(5) Nicholls, P.; Fita, I.; Loewen, P. C. *Adv. Inorg. Chem.* **2001**, *51*, 51−106.
(6) Muira, T.; Suzuki, K.; Takeuchi, H. *J. Mol. Struct.* **2001**, *598*, 79−84.
(7) Berglund, G. I.; Carlsson, G. H.; Smith, A. T.; Szöke, H.; Henriksen, A.; Hajdu, J. *Nature* **2002**, *417*, 463−468.
(8) Gajhede, M. *Biochem. Soc. Trans.* **2001**, *29*, 91−99.
(9) Pramanik, D.; Ghosh, C.; Dey, S. G. *J. Am. Chem. Soc.* **2011**, *133*, 15545−15552.
(10) Karr, J. W.; Akintoye, H.; Kaupp, L. J.; Szalai, V. A. *Biochemistry* **2005**, *44*, 5478−5487.
(11) Faller, P.; Hureau, C. *Dalton Trans.* **2009**, 1080.
(12) Faller, P. *ChemBioChem* **2009**, *10*, 2837.
(13) Dorlet, P.; Gambarelli, S.; Faller, P.; Hureau, C. *Angew. Chem., Int. Ed.* **2009**, *48*, 9273−9276.
(14) Hureau, C.; Coppel, Y.; Dorlet, P.; Solari, P. L.; Sayen, S.; Guillon, E.; Sabater, L.; Faller, P. *Angew. Chem., Int. Ed.* **2009**, *48*, 9522−9525.
(15) Shin, B.-K.; Saxena, S. *Biochemistry* **2008**, *47*, 9117−9123.
(16) Shin, B.-K.; Saxena, S. *J. Phys. Chem. B* **2011**, *115*, 15067−15078.
(17) Drew, S. C.; Masters, C. L.; Barnham, K. J. *J. Am. Chem. Soc.* **2009**, *131*, 8760−8761.
(18) Hou, L.; Zagorski, M. G. *J. Am. Chem. Soc.* **2006**, *128*, 9260−9261.
(19) Azimi, S.; Rauk, A. *Int. J. Alzheimers Dis.* **2011**, *2011*, Article ID 539762 DOI: 10.4061/2011/539762.
(20) Shearer, J.; Szalai, V. *J. Am. Chem. Soc.* **1008**, *130*, 17826−17835.
(21) Feaga, H. A.; Maduka, R. C.; Foster, M. N.; Szalai, V, A. *Inorg. Chem.* **2011**, *50*, 1614−1618.
(22) Veitch, N. C. *Phytochemistry* **2004**, *65*, 249−259.
(23) Watanabe, L.; Ribeiro de Moura, P.; Bleicher, L.; Nascimento, A. S.; Zamorano, L. S.; Calvete, J. J.; Sanz, L.; Pérez, A.; Bursakov, S.; Roig, M. G.; Shnyrov, V. L.; Polikarpov, I. *J. Struct. Biol.* **2010**, *169*, 226−242.
(24) Zhou, Y.; Wang, J.; Liu, L.; Wang, R.; Lai, X.; Xu, M. *ACS Chem. Neurosci.* **2013**, DOI: dx.doi.org/10.1021/cn300231q.
(25) Mayhew, S. G. *Eur. J. Biochem.* **1978**, *85*, 535−547.
(26) Azimi, S.; Rauk, A. *J. Theor. Comp. Chem.* **2012**, *8*, 5150−5158.
(27) Feaga, H. A.; Maduka, R. C.; Foster, M. N.; Szalai, V. A. *Inorg. Chem.* **2011**, *50*, 1614−1618.
(28) Shearer, J.; Szalai, V. A. *J. Am. Chem. Soc.* **2008**, *130*, 17826−17835.
(29) Faller, P.; Hureau, C. *Dalton Trans.* **2009**, 1080.
(30) Hatcher, L. Q.; Hong, L.; Bush, W. D.; Carducci, T.; Simon, J. D. *J. Phys. Chem. B* **2008**, *112*, 8160.
(31) Frisch, M. J.; Trucks, G. W.; Schlegel, H. B.; Scuseria, G. E.; Robb, M. A.; Cheeseman, J. R.; Scalmani, G.; Barone, V.; Mennucci, B.; Petersson, G. A.; Nakatsuji, H.; Caricato, M.; Li, X.; Hratchian, H. P.; Izmaylov, A. F.; Bloino, J.; Zheng, G.; Sonnenberg, J. L.; Hada, M.; Ehara, M.; Toyota, K.; Fukuda, R.; Hasegawa, J.; Ishida, M.; Nakajima, T.; Honda, Y.; Kitao, O.; Nakai, H.; Vreven, T.; Montgomery, Jr., J. A.; Peralta, J. E.; Ogliaro, F.; Bearpark, M.; Heyd, J. J.; Brothers, E.; Kudin, K. N.; Staroverov, V. N.; Kobayashi, R.; Normand, J.; Raghavachari, K.; Rendell, A.; Burant, J. C.; Iyengar, S. S.; Tomasi, J.; Cossi, M.; Rega, N.; Millam, N. J.; Klene, M.; Knox, J. E.; Cross, J. B.; Bakken, V.; Adamo, C.; Jaramillo, J.; Gomperts, R. E.; Stratmann, O.; Yazyev, A. J.; Austin, R.; Cammi, C.; Pomelli, J. W.; Ochterski, R.; Martin, R. L.; Morokuma, K.; Zakrzewski, V. G.; Voth, G. A.; Salvador, P.; Dannenberg, J. J.; Dapprich, S.; Daniels, A. D.; Farkas, O.; Foresman, J. B.; Ortiz, J. V.; Cioslowski, J.; Fox, D. J. *Gaussian 09*, revision A.02; Gaussian, Inc.: Wallingford, CT, 2009.
(32) Cornell, W. D.; Cieplak, P.; Bayly, C. I.; Gould, I. R.; Merz, K. M., Jr.; Ferguson, D. M.; Spellmeyer, D. C.; Fox, T.; Caldwell, J. W.; Kollman, P. A. *J. Am. Chem. Soc.* **1995**, *117*, 5179−5197, http://ambermd.org/.
(33) Clemente, F.; Vreven, T.; Frisch, M. J. In *Quantum Biochemistry*; Matta, C., Ed.; Wiley VCH: Weinheim, 2008; Vol. *1*, pp 61−84.
(34) Vreven, T.; Morokuma, K. In *Continuum Solvation Models in Chemical Physics: From Theory to Applications*; Mennucci, B., Cammi, R., Eds.; Wiley: New York, 2008; Chapter 4, pp 523−534.
(35) Hertwig, R. H.; Koch, W. *Chem. Phys. Lett.* **1997**, *268*, 345−351.
(36) Scott, A. P.; Radom, L. *J. Phys. Chem.* **1996**, *100*, 16502−16513.
(37) Tomasi, J.; Mennucci, B.; Cammi, R. *Chem. Rev.* **2005**, *105*, 2999−3093.
(38) Grimme, S.; Antony, J.; Ehrlich, S.; Krieg, H. *J. Chem. Phys.* **2010**, *132*, 154104−154122.
(39) Raffa, D. F.; Rauk, A. *J. Phys. Chem. B* **2007**, *111*, 3789−3799.
(40) Brault, D.; Rougee, M. *Biochem. Biophys. Res. Commun.* **1974**, *57*, 654−659.
(41) Al-Jaff, G.; Silver, J.; Wilson, M. T. *Inorg. Chim. Acta* **1990**, *176*, 307−316.

(42) (a) Liao, M.-S.; Watts, J. D.; Huang, M. J. *J. Comput. Chem.* **2006**, *27*, 1577−1592. (b) Abdurahman, A.; Renger, T. *J. Phys. Chem. A* **2009**, *113*, 9202−9206.
(43) Singh, R.; Grigg, J. C.; Armstrong, Z.; Murphy, M. E. P.; Eltis, J. D. *J. Biol. Chem.* **2012**, *267*, 10623−10630.
(44) The 418 kJ mol^{-1} is the Gibbs free energy for the half reaction: $^1/_2H_2(g) \rightarrow H_{(aq)}^+ + e^-$. It can be obtained from adding $\Delta_f G^\circ_{(g)}(H^+)$ = 1517 kJ mol^{-1}, $\Delta G_{solv}(H^+)$ = −1107 kJ mol^{-1}, and the factor to change the $H_{(aq)}^+$ reference state to 1 M, $-RT \ln(1/24.6)$ = 8 kJ mol^{-1}. Additionally, $\Delta_f G_{(g)}(H^+)$ = 1517 kJ mol^{-1} is computed from the $\Delta_f G^\circ_{(g)}(H)$ = 203 kJ mol^{-1} (ref 36) plus $\Delta_r G^\circ_{(g)}(H^+ + e^- \rightarrow H)$ = 1314 kJ mol^{-1}. Wagman, D. D.; Evans, W. H.; Parker, V. B.; Schumm, R. H.; Halow, I.; Bailey, S. M.; Churney, K. L.; Nuttall, R. L. *J. Phys. Chem. Ref. Data Suppl.* **1982**, *1*, 11.
(45) Balland, V.; Hureau, C.; Saveant, J.-M. *Proc. Natl. Acad. Sci. U.S.A.* **2010**, DOI: 10.1073/pnas.1011315107.
(46) Ma, K.; Clancy, E. L.; Zhang, Y.; Ray, D. G.; Wollenberg, K.; Zagorski, M. G. *J. Am. Chem. Soc.* **1999**, *121*, 8698−8706.
(47) Wood, P. M. *Biochem. J.* **1988**, *253*, 287−289.
(48) Mayhew, S. G. *Eur. J. Biochem.* **1978**, *85*, 535−547.